Biol. Cybern. 74, 427–437 (1996)

Biological Cybernetics

Identification of the nonlinear state-space dynamics of the action-perception cycle for visually induced postural sway

M.A. Giese[1], T.M.H. Dijkstra[2,*], G. Schöner[1,], C.C.A.M. Gielen[2]**

[1] Institut für Neuroinformatik, Ruhr-Universität Bochum, ND04, D-44780 Bochum, Germany
[2] Department of Medical Physics and Biophysics, University of Nijmegen, P.O. Box 9101, NL-6500 HB Nijmegen, The Netherlands

Received: 8 November 1995 / Accepted in revised form: 23 January 1996

Abstract. Human subjects standing in a sinusoidally moving visual environment display postural sway with characteristic dynamical properties. We analyzed the spatiotemporal properties of this sway in an experiment in which the frequency of the visual motion was varied. We found a constant gain near 1, which implies that the sway motion matches the spatial parameters of the visual motion for a large range of frequencies. A linear dynamical model with constant parameters was compared quantitatively with the data. Its failure to describe correctly the spatiotemporal properties of the system led us to consider adaptive and nonlinear models. To differentiate between possible alternative structures we directly fitted nonlinear differential equations to the sway and visual motion trajectories on a trial-by-trial basis. We found that the eigenfrequency of the fitted model adapts strongly to the visual motion frequency. The damping coefficient decreases with increasing frequency. This indicates that the system destabilizes its postural state in the inertial frame. This leads to a faster internal dynamics which is capable of synchronizing posture with fast-moving visual environments. Using an algorithm which allows the identification of essentially nonlinear terms of the dynamics we found small nonlinear contributions. These nonlinearities are not consistent with a limit-cycle dynamics, accounting for the robustness of the amplitude of postural sway against frequency variations. We interpret our results in terms of active generation of postural sway specified by sensory information. We derive also a number of conclusions for a behavior-oriented analysis of the postural system.

1 Introduction

Postural control has been studied intensively over the past two decades (Nashner and McCollum 1985), not only because of its clinical relevance (Maki et al. 1987) and relation to motion sickness (Riccio and Stoffregen 1991) but also because postural control is a basis for voluntary motor behavior (for a review see Massion 1992) and can be regarded as an example of multisensory integration (Dichgans and Brandt 1978). The conventional method of analysis identifies contributions to postural control with functions which are independent of the overall task or behavior. For instance, the contribution made by the biomechanical properties of the system, the contribution of vision, and of the vestibular system have been distinguished. In this picture the role of an individual sensory system is to act as an input signal for an otherwise passive postural control system. The system components are conceptualized as separable and well-defined units. Each is characterized by individual behavioral characteristics that may be described by a constant transfer function between adequate input and output variables. Vision, for instance, has been described as an external driving force acting on the postural control system which is behaving like an inverted pendulum or driven second- or third-order linear system in order to explain the postural sway induced by a moving visual environment (Lestienne et al. 1977; Talbott 1980; Ishida and Miyazaki 1987; van Asten et al. 1988b).

This approach seems to be problematic when the postural control system does not only react passively to changes in the sensory channels. Changes in the system dynamics by adaptation may occur, or the system may actively self-generate motor activity which is only loosely coupled to the driving visual stimulus. Deviations from the response properties of a passive linear system have been observed, for instance by Maioli and Poppele (1991) and by Talbott and Brookhart (1980), who varied the temporal frequency of mechanical perturbations, leading to the interpretation of postural behavior as an adaptive control process (Schuster and Talbott 1980). Dijkstra et al. (1994a) varied the visual distance from a moving visual environment and found deviations from the gain predicted by a passive linear model (Schöner 1991) for the effect of visual flow on postural control. More direct evidence for active generation of postural sway was obtained when the relative timing of sway and visual motion was analyzed as a function of the frequency of visual motion (Dijkstra et al. 1994b). It was found that

* *Present address:* Department of Psychology, University of Pennsylvania, 3815 Walnut Street, PA 19104 Philadelphia, USA
** *Present address:* CNRS-LNC, 31, Chemin Joseph Aiguier, F-13402 Marseille Cedex 20, France
Correspondence to: M. Giese

temporal coherence between stimulus and postural response is lost at higher frequencies and relative coordination in the sense of von Holst (1937) was observed. A dynamical system analysis of the relative phase showed that this effect is incompatible with an account based on a simple linear passively driven postural control system. More generally, work in several related fields points toward a more active role of the postural control system. Different postural motor strategies are selected in response to external and internal constraints (Nashner and McCollum 1985). Posture is involved in an anticipatory compensation of perturbations induced by voluntary movement (Massion 1992), and central set effects on posture have been postulated (e.g., Horak et al. 1989).

In the light of these findings, approaches which assume modules of the postural control system that are fixed identifiable entities, appear problematic. The question therefore arises how the postural system might alternatively be conceptualized and analyzed. We will address this problem here by starting from two basic assumptions: (1) Analysis is made in terms of variables that characterize the action-perception cycle in the intact behavior. These variables – for instance the position of the center of mass in the world – are usually multi-sensory, highly integrated quantities seen from the point of view of individual sensory channels. (2) The dynamics of the action-perception cycle is identified in a situation in which the system shows stable and reproducible postural behavior in relation to its environment. As the behavioral situation changes (e.g., if the available sensory information is manipulated), this dynamics may change. This change has to be identified rather than predicted. The result of such an analysis is a dynamical system that links the dynamical properties of the system within one behavioral state, for instance responses to external perturbations and the spontaneous behavior in the absence of such perturbations. When a simple dynamics describing the system in all behavioral situations seems not to exist we propose to proceed in two steps. First the dynamics in the individual behavioral situations has to be identified. In a next step these individual dynamics may be embedded into a more complex dynamical system, which, for example, may allow bifurcations between qualitatively different behaviors.

To perform such a 'behavioral' analysis we refer to an experiment in which subjects stood on firm ground while being presented with an oscillatory moving visual environment (Dijkstra et al. 1994a,b). The frequency dependence of gain and visual expansion rate are reported. By fitting gain and phase with a constant-parameter linear dynamical model we expose the shortcomings of an analysis by decomposition into passive invariant modules of postural control (Sect. 3). We then develop a method for fitting linear (Sect. 4) and nonlinear (Sect. 5) models directly to the time series of postural and visual motion, so that the dynamics can be determined independently for each behavioral condition.

2 Experimental methods

We briefly summarize the experimental paradigm and methods. For more details see Dijkstra et al. (1994a). Subjects stood approximately 50 cm in front of a large translucent screen on which computer-generated visual displays were projected. A real-time feedback architecture made it possible to control the visual input on the optic array independently of the postural reaction. The precise temporal control of the stimuli makes the data well suited for an analysis of the dynamical properties of the visually induced postural sway. The stimuli simulated a fronto-parallel wall covered with 140 dots at a mean distance of 50 cm. The wall moved sinusoidally in forward-backward direction with frequencies of 0.05, 0.1, 0.2, 0.3, 0.4 and 0.5 Hz. The amplitude of visual motion co-varied with frequency so as to keep the mean absolute velocity of the wall constant. The amplitudes (10, 5, 2.5, 1.67, 1.25 and 1 cm) were near the threshold for conscious motion perception. This minimizes nonlinear effects caused by physical limitations of the motor effectors or geometric distortions of the stimuli. All conditions contained two perturbations[1] of the phase of the sinusoidal stimulus motion of 180 deg at the point of maximum velocity. Each condition was repeated six times. Each trial lasted for 140 s and the first 20 s used for adaptation were not stored. Six subjects with normal or corrected-to-normal vision were tested in all conditions. Three of the subjects were familiar with the purpose of the experiment.

3 Analysis in terms of constant parameter models

To characterize the postural system in terms of different invariant modules a typical assumption is that the postural control system is a second-order linear dynamical system or filter, driven by sensory input (Schuster and Talbott 1980; Ishida and Miyazaki 1987; van Asten et al. 1988b; Schöner 1991). Such models can be compared with experimental data by measuring the dependence of postural sway measures such as gain, phase and root mean square on the manipulated experimental parameter, such as frequency and amplitude of an external perturbation. Since it is assumed that the model parameters remain constant for different external stimulations, their values can be determined by fitting the experimentally observed dependencies. If this fitting is successful, the invariant modules of the control system have been identified and, in principle, predictions arise as to the response to other types of stimulation. This is the classical program of analysis. In this section we follow that program to highlight in which form it fails.

To set the stage for such an analysis we refer to the model by Schöner (1991). The model postulates a second-order dynamical system to describe the postural control system which is driven by the visual expansion rate. The model addresses postural sway in behavioral variables that are directly accessible to observation, such as the position of the eye in the world and the retinal expansion rate. Because both variables are plausibly available to physiological mechanisms (although the first involves a nontrivial integration of sensory information), this model can be used as a representative of the classical approach. At the same time, however, we shall show in Sect. 4 that the model is more adequately interpreted and applied within a behavior-oriented analysis.

We first derive the predictions of the model for the dependence of gain and phase on frequency (Sect. 3.1) and then

[1] An exception is the 0.05 Hz condition, which contained only one perturbation because of the low number of cycles within an experimental trial.

determine the parameters by fitting these predictions to our experimental results (Sect. 3.2).

3.1 Linear dynamic model of postural coupling to vision

The position, x, of the eye in the inertial world is assumed to be governed by a dynamical system of the form:

$$\ddot{x} = -\alpha\,\dot{x} - \omega_0^2\,x + \sqrt{Q}\,\xi_t - c_{\text{env}}\,e(x,t) \qquad (1)$$

In the present analysis, the first three terms are interpreted as expressing the capability of the postural system to stabilize the position of the eye in the world in the absence of visual information (e.g. as observed under eyes-closed conditions). The parameter α is the damping coefficient and ω_0 the eigenfrequency of the system. White noise, ξ_t, [with zero mean and autocorrelation function $< \xi_t \xi_{t+\tau} >= \delta(\tau)$], accounts for the occurrence of fluctuating postural sway in the absence of visual information. Q determines the strength of the noise.

The last term singles out the contribution of vision to posture by coupling the expansion rate of the optical flow in the visual scene additively to the dynamics. This is a scale invariant variable that includes both the contribution of sway and the movement of structures in the environment to optic flow. If $D(t)$ is the distance of the visual scene from the origin of the coordinate system in which sway is measured the expansion rate is defined as $e(x,t) = -(\dot{D} - \dot{x})/(D - x)$. We shall consider sinusoidally moving scenes at a mean distance, D_0, which is assumed to be much larger than the oscillation amplitude, D_r, yielding formally $D(t) = D_0 + D_r \sin(\omega_D t)$, where $\omega_D/(2\pi)$ is the frequency of the sinusoidal motion of the scene. If D_0 is also much larger than the sway amplitude the time dependence in the denominator of e can be neglected yielding the dynamics:

$$\ddot{x} = -\tilde{\alpha}\,\dot{x} - \omega_0^2\,x + \sqrt{Q}\,\xi_t + (c_{\text{env}}\,D_r\omega_D/D_0)\,\cos(\omega_D t) \quad (2)$$

Here, $\tilde{\alpha} = \alpha + c_{\text{env}}/D_0$ is the effective damping containing both the nonvisual contribution, α and the visual contribution, c_{env}/D_0. For purposes of quantitative identification of the model parameters we generalize the equation slightly by allowing an additional constant phase delay ψ, between driving force and response:

$$\ddot{x} = -\tilde{\alpha}\,\dot{x} - \omega_0^2\,x + \sqrt{Q}\,\xi_t + (c_{\text{env}}\,D_r\omega_D/D_0)\,\cos(\omega_D t - \psi) \quad (3)$$

By Fourier transformation of the deterministic part of (3) the transfer function $H(i\omega) = G(\omega)\,\exp(i\varphi(\omega)) = X(i\omega)/U(i\omega)$ is obtained, where $X(i\omega)$ and $U(i\omega)$ are the Fourier transforms of x and the oscillatory component of visual distance $u(t) = D_r\,\sin(\omega_D t)$. The gain and the phase are then given by:

$$G(\omega_D) = \frac{\omega_D c_{\text{env}}}{D_0\,\sqrt{(\omega_0^2 - \omega_D^2)^2 + (\tilde{\alpha}\,\omega_D)^2}} \qquad (4)$$

$$\varphi(\omega_D) = \arctan\left(\frac{\omega_0^2 - \omega_D^2}{\tilde{\alpha}\,\omega_D}\right) - \psi. \qquad (5)$$

For the model without delay ($\psi = 0$) the stationary amplitude of the expansion rate on the optic array can be reconstructed from (1), cf. Dijkstra et al. (1994a):

$$E(\omega_D) = (\omega_D\,D_r/D_0)\,\sqrt{1 - \frac{(\tilde{\alpha}^2 - \alpha^2)\,\omega_D^2}{(\omega_0^2 - \omega_D^2)^2 + (\tilde{\alpha}\,\omega_D)^2}} \qquad (6)$$

By transforming the dynamics (3) into polar coordinates, stability measures of the stationary oscillatory solutions have been derived and compared with experimental results (Schöner 1991; Dijkstra et al. 1994a, b).

3.2 Quantitative comparison with experiment

3.2.1 Methods. Data were smoothed with a Gaussian filter (standard deviation 0.64 s for frequency condition 0.05 Hz, 0.36 s for 0.1 Hz, and 0.18 s for frequency conditions 0.2–0.5 Hz). Angular expansion rate was calculated as a time series from the recorded stimulus motion and subjects' eye position (cf. Dijkstra et al. 1994a) and the amplitude of this time series was determined from the spectrum at the driving frequency. To ensure stationarity, periods of 8 s after the phase perturbations of the stimulus motion (cf. Sect. 2) were excluded from the spectral analysis and the determination of gain and phase. For the spectral analysis we used a Welch procedure (Marple 1987) with factor 3 zero padding and averaging over seven segments. Gain and stationary phase were calculated using a procedure described in Dijkstra et al. (1994a). It is based on the detection of significant extrema of the visual and response signal using an adaptive peak-picking algorithm. The gain can then be simply computed as the ratio of mean amplitudes at the significant extrema of the driving signal and of the measured response signal. Local cycle times are determined by computing the temporal distance between subsequent extrema yielding local frequency estimates by taking the reciprocals. The values were averaged over four different extrema types: peaks and valleys of position and of velocity signals. More details about the algorithms and about the calculation of the phase of the transfer function can be found in Dijkstra et al. (1994a, b). Typically the results of gain and phase as calculated by the method of Dijkstra et al. (1994a, b) were highly correlated with the results from a classical spectral analysis using the Welch procedure (for instance $r = 0.67 \ldots 0.95$, mean 0.88, $t > 4.4$ for gain). The procedure based on significant extrema seemed to be more robust for our data and remains applicable for nonlinear systems.

To test the adequateness of linear dynamical models with constant parameters we fitted the experimentally determined transfer functions with the functional forms predicted from the model. These fits minimized the deviations of the predicted values of the transfer function from the data in square-norm in the Gaussian plane. Using a nonlinear Levenberg-Marquardt minimization procedure (Press et al. 1988) we minimized a functional of the form $S = \sum_i \left[(G_i - G(\omega_{D,i}))^2 + K(\varphi_i - \varphi(\omega_{D,i}))^2\right]$, where $\omega_{D,i}$ is the driving frequency of trial i, and G_i and φ_i are the measured values of gain and phase. Choosing $K = 0.15$ we obtained approximately equal qualities of the fits for gain and phase with the resulting parameter set. For illustration purposes and to check the consistency of the fitted model we also performed fits without an additional phase delay ψ and fits based on a stepwise procedure. In the latter we either fitted the phase from (5) first and then used (4) to determine c_{env} ('fits starting from the phase'), or we used the gain equation (4) for the determination of all parameters and used (5) only to predict the frequency dependence of the phase and to compare it with the measured dependency ('fits starting from gain'). The qualities of the fits were evaluated by calculating the percentages of the total variance of the measured gain and phase which was explained by the fitted models.

3.2.2 Results and discussion. In all plots showing the results separately for the six subjects the order of presentation (from left to right) is: GS, MG, CG, CK, AM, JO. All significance tests in the paper refer to a significance level of 5%.

The amplitude of sway as a function of driving frequency is shown in Fig. 1, where the gain has been plotted as a function of the frequency of the visual scene. The most striking overall result here is that amplitude changes only weakly with frequency, with an increase for low frequencies, and

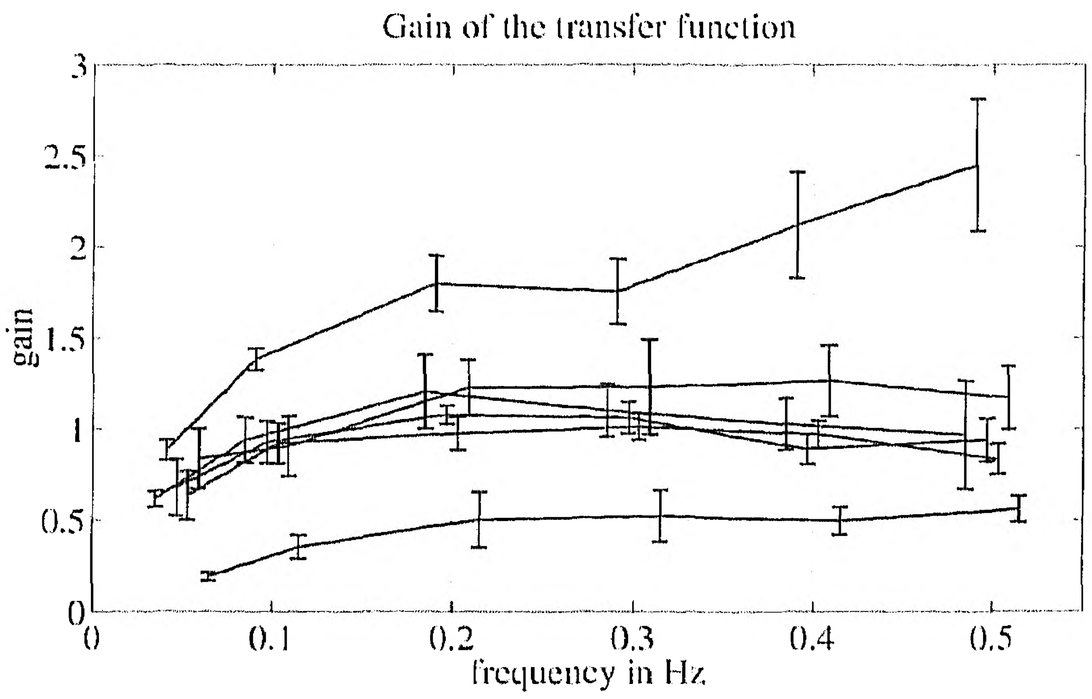

Fig. 1. Gain of transfer function as a function of driving frequency for six subjects.The error bars mark the standard deviations over the repetitions of the experimental conditions. The sequence of presentation of the results of the subjects is always (from *left* to *right*): GS, MG, CG, CK, AM, JO

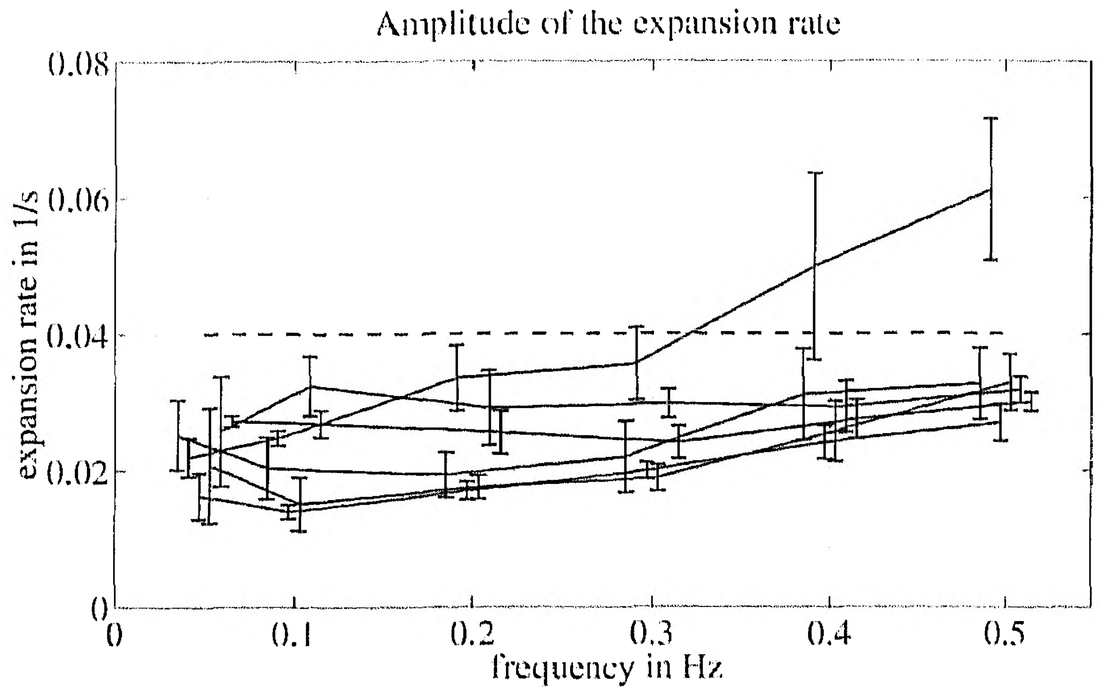

Fig. 2. Amplitude of the reconstructed expansion rate on the optic array as a function of driving frequency for six subjects. The *dash-dotted line* marks the amplitude of the expansion rate for a stationary observer placed at distance D_0 in front of the stimulus

a plateau at higher frequencies for all subjects except MG. There is little evidence for a resonance type maximum near typical sway frequencies (of about 0.1–0.2 Hz). Moreover, a gain near 1 indicates that postural sway matches the movement of the visual scene in amplitude. Specifically, the gain showed a significant dependence on driving frequency for all six subjects ($F(5, 30) > 5.8$). For three subjects the frequency dependence of gain was not significant for frequencies *above* 0.1 Hz ($F(3, 20) < 1.5$).

The amplitude of the reconstructed angular expansion rate of the optical flow is presented in Fig. 2. For all subjects except one the expansion rate varies with driving frequency and is slightly smaller in the middle frequency range. The frequency effect is significant in four cases ($F(5, 30) > 4.8$). One subject (MG) shows a continuous significant increase towards higher frequencies ($F(5, 30) = 22.9$). In the figure the dashed horizontal line indicates the amplitude of the expansion rate for a stationary observer at the resting position. Evidently, all subjects are able to reduce the amplitude of the retinal optical flow through the compensatory postural movement by an amount of between 20% and 60%. This is consistent with a gain near 1 and a phase which does not strongly deviate from zero (see below). Both may be interpreted as a tendency of the system to match the spatiotemporal structure of the motion of the environment yielding to a reduction of the retinal optical flow. An exception is subject MG, who tends to produce high-amplitude oscillations in the upper frequency range which even enhance the optical flow beyond the resting-observer level. However, the frequency dependence of the amplitude of expansion rate rules out a simple expansion-rate thresholding mechanism, through which expansion rate would be kept just below a maximal value. This interpretation is corroborated by the results of Dijkstra et al. (1994a), who found that the expansion-rate amplitude strongly decreases with visual stimulus distance D_0, and by the results of Paulus et al. (1989), who found a better stabilization of posture than would be predicted from the visual object-motion thresholds.

The two results on expansion rate and gain suggest that a description of this system in terms of peripheral sensory variables (such as the retinal slip) is not simple. The system description has to be adapted in a more or less complex way if external variables such as distance or stimulus frequency are changing. An alternative description of the system is obtained by: (1) Characterization of the external stimulus motion and the postural sway in a single coordinate system (the external inertial frame in our case). (2) Analysis of the system in terms of the complete action-perception cycle revealing a tendency of the system to match the postural movement and the environmental motion in amplitude. This description is simpler in the sense that it remains invariant when parameters outside the system, such as distance or frequency, are changing.

Figure 3 (middle part) shows the phase of the transfer function. Superficially, the typical structure of a linear driven system is apparent, with a phase lead at low frequencies, in-phase near resonance and a phase lag at high frequencies (for details see Dijkstra et al. 1994b). However, this phase effect is much less accentuated than expected, very like the rather muted resonance effect in the gain variable. To make this point explicit, we fitted the parameters of the model (3) to the measured transfer functions. Without additional phase delay ($\psi = 0$) corresponding to the original model by Schöner [1991; cf. (1)] we found that no consistent fits were possible. Figure 3 demonstrates this inconsistency, comparing the fits starting from the gain and from the phase for a typical subject. Fitting the frequency dependence of the gain correctly leads to a deviation of the predicted phase from the data and vice versa. The parameter values obtained from both fits differed by factors up to 4 and were at times outside the range determined as consistent with the relative phase dynamics (cf. Dijkstra et al. 1994b). When an additional phase delay was permitted, the results did not improve and the fit quality became very variable. The fitted parameters predicted much stronger frequency dependence of expansion rate according to equation (6) than was experimentally observed (cf. Fig. 3, bottom). The low fit quality is also reflected in the low explained variances for the combined fits – on average 40%.

We remark that almost any frequency dependency of the transfer function could be fitted by a linear dynami-

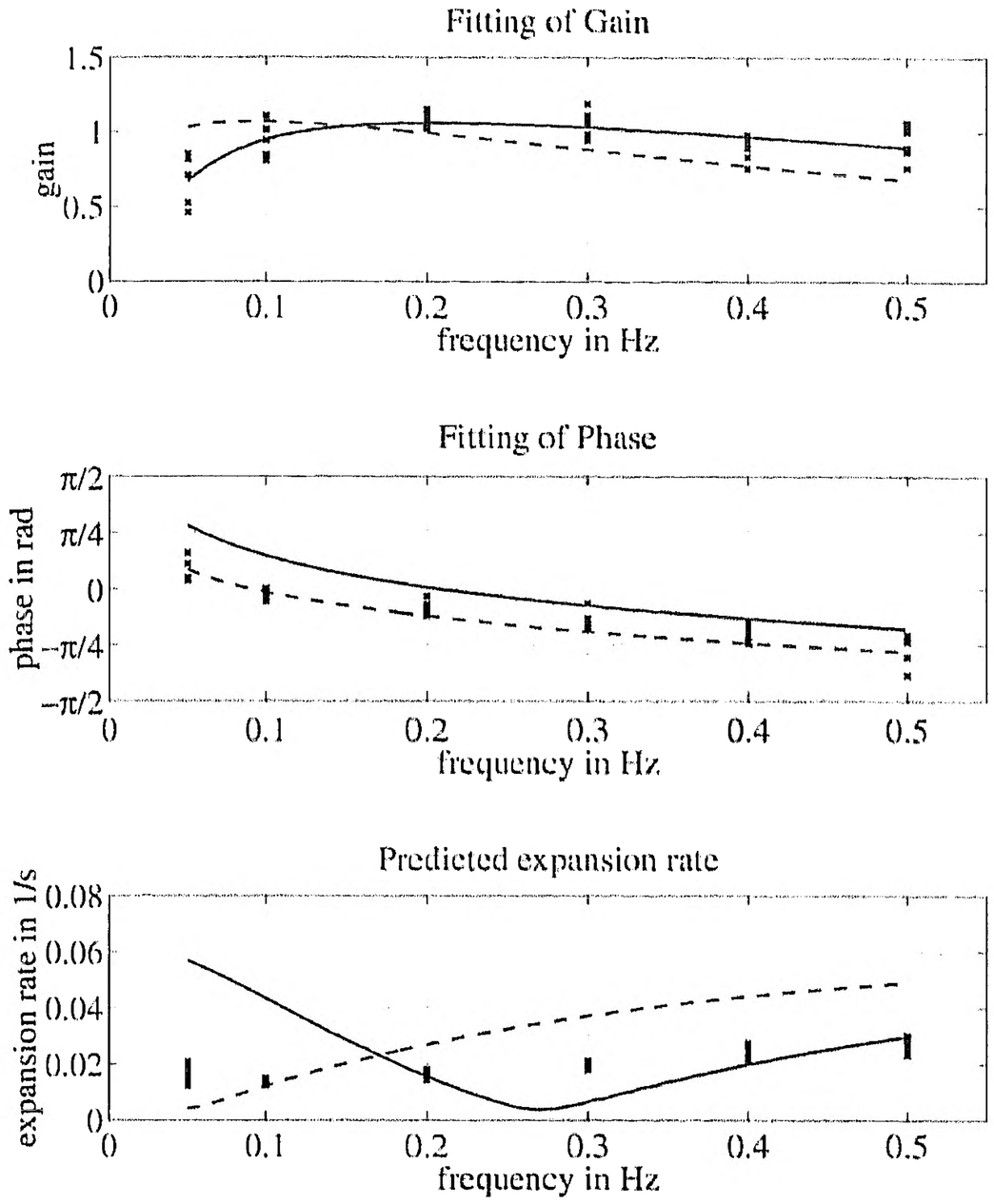

Fig. 3. Fitting of transfer function (*top*, gain; *middle*, phase) with constant parameters: The *crosses* mark the measured values for gain and phase for a typical subject. The *lines* indicate the predicted shape of the transfer function of a linear driven system with the fitted parameters. The *continuous line* refers to a fit which started from the gain data and fitted the phase in a second step. The *dashed line* was obtained with the fit starting from the phase data and gain was fitted in the second step. The *bottom panel* shows the amplitudes of the visual expansion rates that would be predicted from the fitted models. If the real system were linear and had constant parameters the two fits should not differ significantly

cal system with appropriately high order.[2] Because in other studies using information criteria for a model order estimation orders of 2–3 have been found to be appropriate for the linear approximation of the posture system (Ishida and Miyazaki 1987) we did not investigate higher-order models. The second-order model was also consistent with the results on visually induced postural sway by van Asten et al. (1988b). The deviations from a second-order linear system found by Dijkstra et al. (1994a, b) point to essentially nonlinear components of the dynamics and can not be simply accounted for by increasing the order of the linear model. This led us to the investigation of adaptive and nonlinear systems rather than of higher-order linear systems.

4 Linear dynamic model with adaptive parameters

Two aspects of the dynamic properties of this action-perception system remain unclear: (1) The constant-parameter linear model fails to account for the change in sway amplitude and phase with frequency: The sway pattern produced is more tightly linked in space and time to the motion of the visual scene than expected for a passively driven system. We had reported a similar tendency earlier in experiments that varied the distance to the visual scene (Dijkstra et al. 1994a). The first deviation could be accounted for by changing the order of the linear system. For the second deviation at least an adequate distance-dependent modification of the visual coupling would be required. (2) Visual motion continues to affect the space-time structure of postural sway even in a regime where temporal coherence between these signals is lost (through an instability of the relative phase dynamics). This was shown in an earlier analysis of the relative phase between sway and visual motion (Dijkstra et al. 1994b) and can not be accounted for within the picture of a simple linear passively driven system at all.

One obvious alternative explanation for these deviations is that the parameters of the postural system depend on the frequency of visual motion, ω_D (and probably on the distance from the stimulus). In the model this would mean that even those parts of the model which are not directly coupled to optic flow are affected by optic flow properties. In other words, an adaptation process could change $\omega_0 = \omega_0(\omega_D)$, $\tilde{\alpha} = \tilde{\alpha}(\omega_D)$, and $c_{\text{env}} = c_{\text{env}}(\omega_D)$ in such a way as to stabilize further the system in the visual world. This idea was tested very directly by determining the parameters of the dynamical model separately for each trial through a fit of the experimentally observed postural sway and visual motion trajectories. Such a fit was possible, because the data contained well-defined transients induced by the phase perturbations of the visual flow.

4.1 Methods

The fit of the linear system model was embedded in the complete nonlinear system identification algorithm sketched in Sect. 5. First slow postural drift was removed from the data by subtracting an average signal obtained by Gaussian filtering (standard deviation 2.3 s for conditions 0.3–0.5 Hz, 3.4 for 0.2 Hz, 6.8 for 0.1 Hz and 16 s for 0.05 Hz conditions). High-frequency noise was removed by Gaussian filtering (standard deviation 0.3 s for conditions 0.2–0.5 Hz, 0.6 s at 0.1 Hz and 1.2 s at 0.05 Hz conditions). The data were divided into segments of length 40 s (50 and 70 s, respectively, for the two lowest driving frequencies) each starting with a phase perturbation of visual motion. Velocity traces were obtained by numerical differentiation. The variability of the results depended only weakly on the filter parameters and beyond a minimum value not on segment length. A crucial problem for fitting trajectories in the driven linear system is to resolve ambiguities that result from linear dependence between various terms of the model. A solution is to separate stationary and transient parts of the data. This was achieved by fitting the particular solution of the differential equation (a periodic function at the driving frequency) to the stationary parts of the data (Fig. 4, top). This function was then extrapolated back in time into the non-stationary epochs, and the transient part of the data was obtained by subtraction (Fig. 4, middle). To this transient part was fitted the solution of the autonomous part of the differential equation. The coupling parameters then were determined by fitting the complete solution[3] (Fig. 4, bottom). A small part of the data (3%) had to be excluded from the analysis because it did not contain any stimulus-related behavior at all.

The identification procedure was evaluated by simulating data sets using a fifth-order Runge-Kutta method for models with realistic parameter settings and Gaussian white noise. The eigenfrequency estimation turns out

[2] This is simply a consequence of the Weierstrass approximation theorem stating that any smooth function can be approximated arbitrarily well by a polynomial of sufficiently high order.

[3] For linear systems this method is basically identical to Prony's method for linear system identification (Halfon et al. 1979). We found that the method can be generalized to weakly nonlinear oscillatory systems as well. In this case the separation of transient and stationary data parts holds only in an approximate sense.

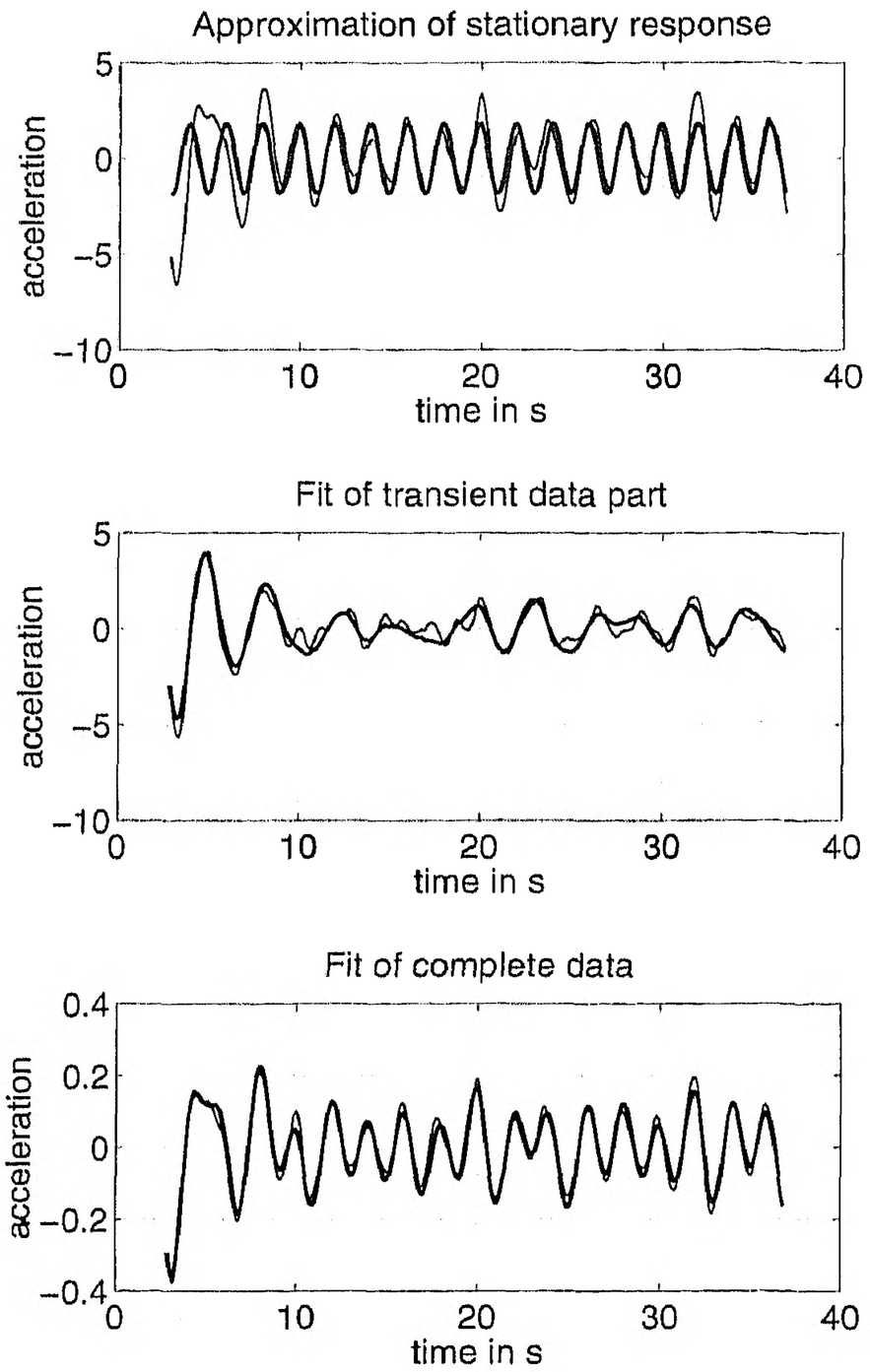

Fig. 4. The separation of transient and stationary parts of the data for simulated data. *Top:* The stationary part of the data trajectory (*thin line*) is approximated by a function system containing harmonics of the driving frequency up to an order of 9. The approximation (*thick line*) allows backward extrapolation of the stationary solution into the nonstationary data segment after the perturbation at the beginning of each trajectory. The stationary solution is scaled to a mean amplitude of 1. *Middle*: The transient part of the data (*thin line*) is calculated by subtraction of the approximated stationary solution from the trajectory. The autonomous solution can be fitted (*thick line*). This yields initial values for the fits of the parameters $\tilde{\alpha}$ and ω_0. *Bottom*: The coupling constants and the nonlinear parameters are determined from the fit of the complete trajectory by a stepwise regression procedure. This is combined with a nonlinear optimization procedure for $\tilde{\alpha}$ and ω_0. The fit (*thick line*) and the original data (*thin line*) are shown in nonscaled coordinates

to be highly robust. In the presence of substantial noise the estimations for damping and coupling constants become variable and tend to be too small. This might be due to the consistency of noisy trajectories with mainly noise-driven weakly damped model structures. Additionally, the noise deviation of trajectories by chance can be consistent with nonlinearities in the model leading to an unsystematic occurrence of significant nonlinear terms in the nonlinear system identification algorithm (see below). On average this reduces the variance assigned to the linear terms in the fit. The estimated parameters for the linear part of the model hardly differed from the values obtained by using the original system identification algorithm by Kortmann (1988) with and without nonlinear terms.

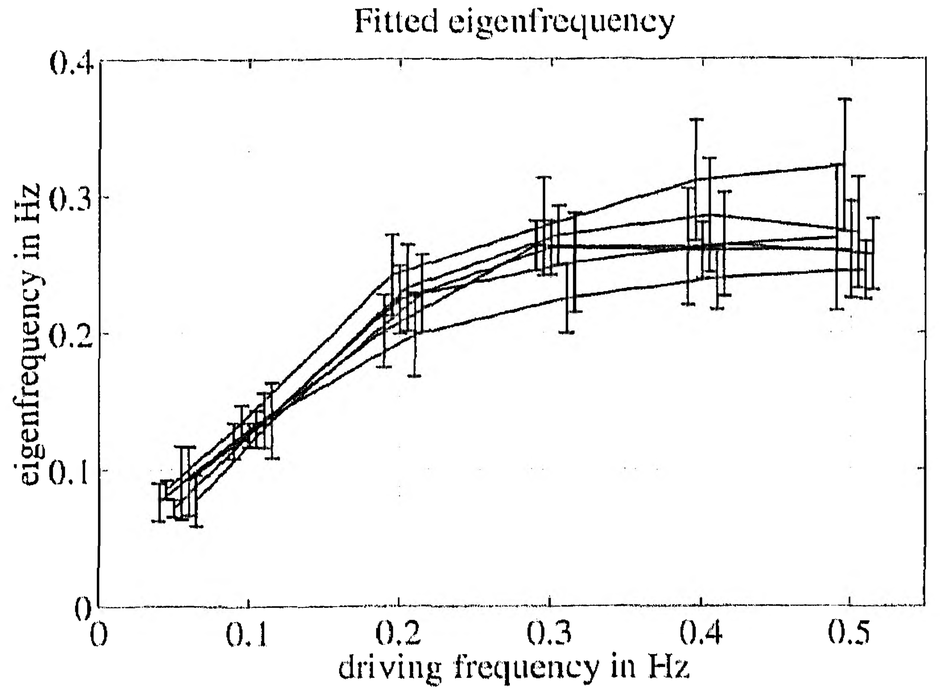

Fig. 5. Fitted eigenfrequency $\omega_0/(2\pi)$ as a function of driving frequency for six subjects. The error bars mark the standard deviations over the repetitions of the experimental conditions. (Order of presentation: GS, MG, CG, CK, AM, JO)

4.2 Results and discussion

Figure 5 shows the fitted eigenfrequency $\omega_0/(2\pi)$ as a function of driving frequency, $\omega_D/(2\pi)$. Up to a driving frequency of 0.3 Hz the eigenfrequency of the postural system matches closely the frequency of visual motion. An exact match is achieved near 0.18 Hz, consistent with the frequency at which relative phase crosses zero (Dijkstra et al. 1994b). The increase is highly significant for all subjects ($F(5, 60) > 43$). At higher driving frequencies the eigenfrequency levels off to a value of approximately 0.25 Hz (0.3 Hz for MG).

The effective damping constant $\tilde{\alpha}$ also exhibits a strong frequency effect as shown in Fig. 6 [significant for five subjects; $F(5, 60) > 5.5$]. For two subjects this damping is small throughout, typically below 0.1 Hz. These subjects showed the lowest temporal stability in the analysis by Dijkstra et al. (1994b). A part of the effect might be due to the underestimation of damping terms at high noise levels. The typical values in the mid-frequency range (between 0.2 and 0.4 Hz) correspond to relaxation times of the relative phase dynamics (cf. Schöner 1991) of 5–10 s, somewhat higher than some of the values measured by Dijkstra et al. (1994b). It is not trivial that such estimates based on very different procedures (extracting relaxation time of relative phase from perturbation trials by direct fit of temporal evolution of relative phase in one case, fitting oscillator model to trajectories in the other case) match at all.[4]

It is very interesting to look at the hypothetical damping constant, $\alpha = \tilde{\alpha} - c_{\text{env}}/D_0$ of the system without stabilization input from the optic array: Fig. 7 reveals that this damping is negative or close to zero for all subjects and strongly decreases to levels as low as -0.5 Hz for high frequencies (even towards -1.5 Hz for MG). Thus the linear dynamics of the postural system without the stabilization by visual input would be unstable.

The coupling to the driving input (Fig. 8) shows a weak increase [significant for four subjects; $F(5, 53) > 3.2$] which

[4] For technical reasons the agreement may be better than it appears, because relaxation time tends to be underestimated in the procedure used by Dijkstra et al. (1994b) (who discarded data segments in which the relative phase fails to return to an attractor after the phase perturbations), while

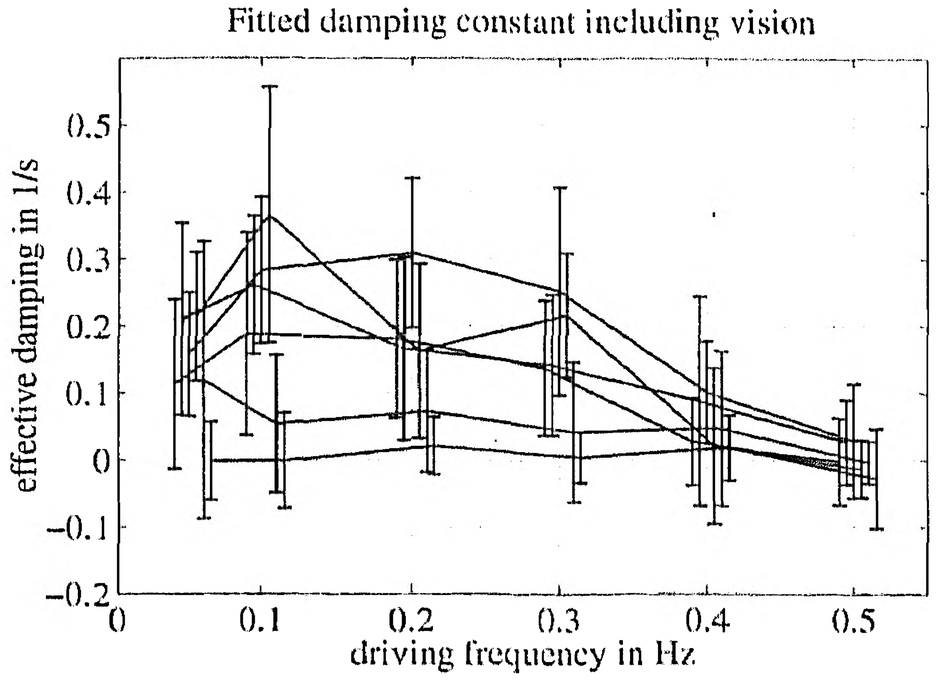

Fig. 6. Effective damping constant $\tilde{\alpha} = \alpha + c_{\text{env}}/D_0$ as a function of driving frequency for six subjects obtained from fitting at trajectory level. This damping constant includes the stabilizing influence of vision

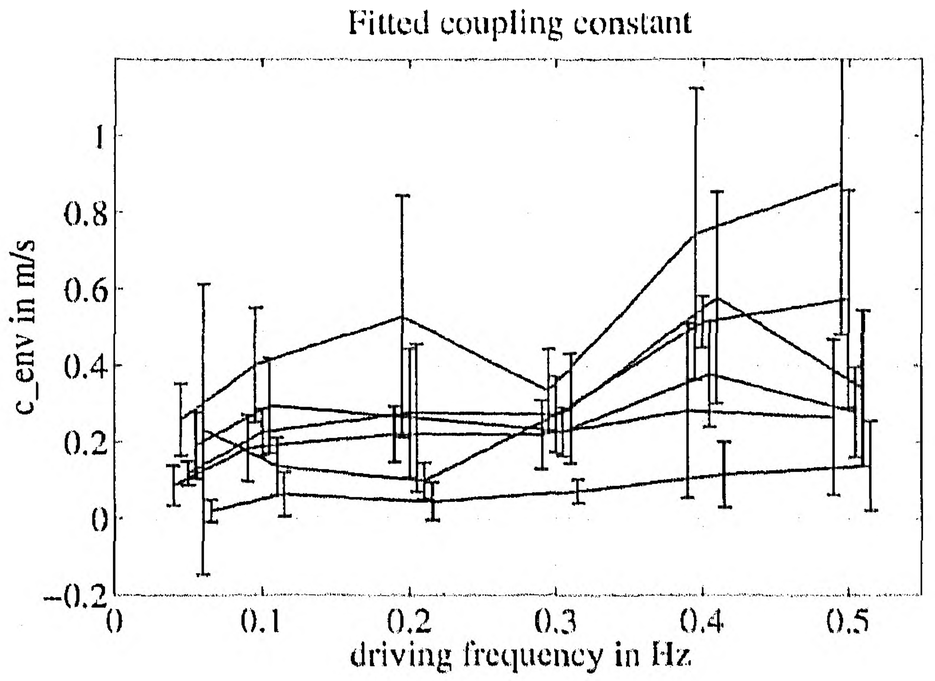

Fig. 8. Fitted coupling constant c_{env} of the coupling to the optic flow as a function of driving frequency for six subjects

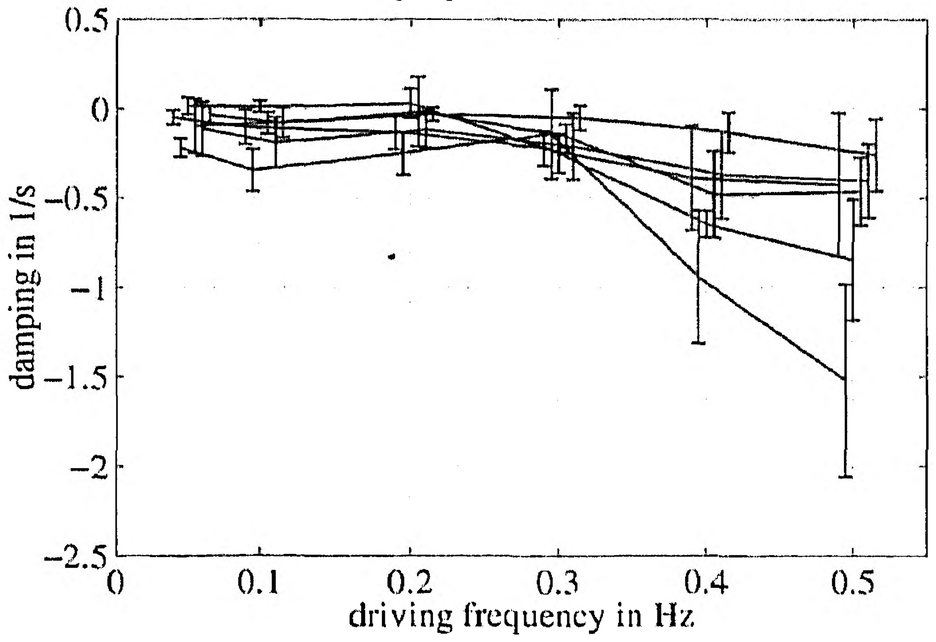

Fig. 7. Corresponding damping constant α, which does not include the stabilizing contribution of vision, as a function of driving frequency for six subjects. The constant is negative indicating that the system would be unstable without the visual driving term $c(x, t)$

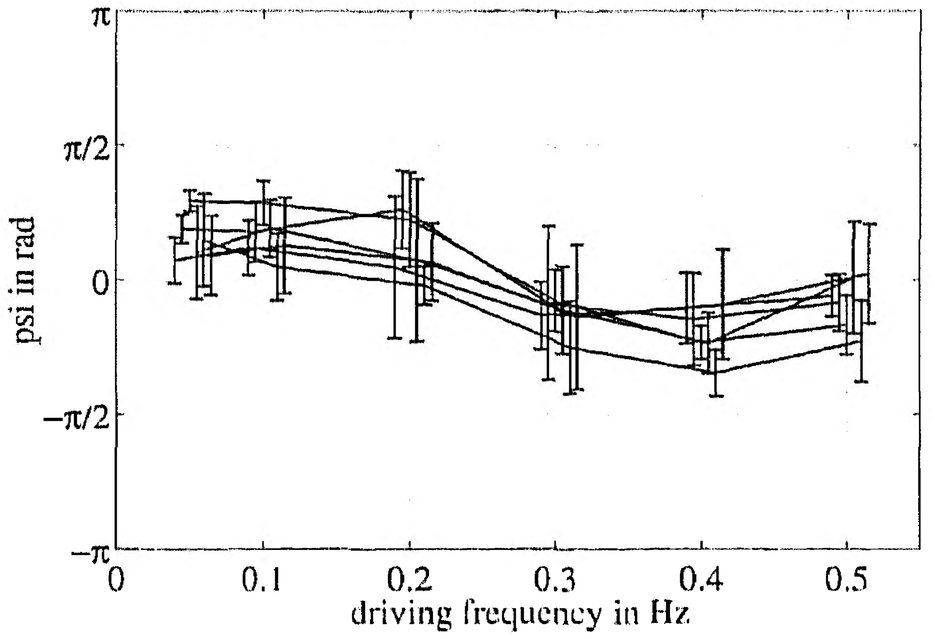

Fig. 9. Fitted phase-shift ψ of the coupling to the optic flow as a function of driving frequency for six subjects

may be interpreted as increasing sensitivity of the system to the visual stimulus when the stability of the postural response is low. This interpretation is corroborated by an analogous analysis of earlier data of Dijkstra et al. (1994a), in which the distance to the visual scene was varied. We fitted trajectories from that experiment using the same procedure. For large distances the effective damping coefficient tended to decrease and the coupling to the expansion rate tended to increase (significantly for three of four subjects).

The frequency dependence of the parameter ψ [significant for all subjects; $F(5, 51) > 2.6$] is not consistent with a purely driven system (Fig. 9). However, that phase shift is moderate, typically below 25 deg. Its nonmonotonic dependence on frequency shows that it cannot be interpreted as a constant time delay in the sensory-motor loop. Effectively, it reduces the dependence of the total phase delay of the system on frequency compared with a constant parameter system.

The estimated noise level $\sqrt{Q}$ is constant over the entire driving frequency range, with values in the range 2.2–3.2 $\sqrt{\text{Hz}}$. This shows that all frequency-dependent variance components have been extracted from the data by the system identification algorithm.

We compared the fitted models with our previous results in two ways. First, we correlated the measured values of the transfer function (Dijkstra et al. 1994b, and this paper) with the values predicted from (4) and (5) if the fitted parameters are used. The predicted gain is too small for some of the subjects, especially for the high driving frequencies. The predicted gain nevertheless account for a considerable part of the variance of the measured gains (53–92%, mean 72.5%). This is a much higher consistency with the measured gain than can be obtained with a constant-parameter model. The correlations between predicted and measured gain range from −0.24 to 0.37 (mean 0.1) and are significant for two of the subjects ($t > 2$, $N > 54$). A low correlation is expected since the gain does not change much with frequency. The phase of the transfer function corresponds very well to the predicted characteristics which is reflected in high correlations (significant for all subjects; $r = 0.67 \ldots 0.86$, mean 0.76; $t > 6.1$, $N > 48$). The explained variance for the phase is high for five subjects (61–84%, mean 72%). For one subject (AM) the measured phase is much weaker dependent on frequency in the high-frequency range than for the other subjects. This deviation is not found for the predicted phase leading to a low explained variance (21%).

damping tends to be underestimated for noisy data in our procedure (see above).

A second test was to predict the parameters of the sine circle map which was fitted to the data by Dijkstra et al. (1994b) using an Euler approximation of the relative-phase differential equation from the averaged nonlinear dynamics in polar coordinates. This is only a very coarse approximation. In principle the sine circle map must be derived from the two-dimensional Poincaré map of an oscillatory system by elimination of the amplitude variable (Bohr et al. 1984). We found good correspondence for the local and global stability measures derived from the sine circle map in Dijkstra et al. (1994b). The correlations between the global stability measure γ obtained from a relative phase analysis and the predicted measure from the fitted models were significant for all subjects ($r = 0.66 \ldots 0.80$, mean 0.72, $t > 5.8$, $N > 34$). The correlations for the local stability measure λ were lower and positive for five subjects ($r = -0.21 \ldots 0.25$, mean 0.11, all not significant). Again the low correlation is expected because the local stability measure, which is directly related to the relaxation time, does not vary much with frequency (cf. Dijkstra et al. 1994b). For all subjects there was a highly significant nearly one to one correspondence between fitted eigenfrequency and the mean of the local response frequency calculated in the relative phase analysis ($r = 0.88 \ldots 0.93$, $t > 14$, $N > 59$).

This comparison shows that the system has a well-defined dynamics, so that assessing its properties from rather different sides based on different measures leads to a consistent description.

5 Nonlinear dynamic model

In view of the low stability of the postural state in the linear model ($\tilde{\alpha}$ small, α negative) the question must be addressed as to whether the dynamics is essentially nonlinear. Specifically, the negative damping of the model without the visual contribution could lead to a bifurcation of the postural dynamics stabilizing a new, nonlinear solution – for instance, a limit cycle. This would explain the robustness of the response amplitude over a wide frequency regime. An answer to this question can be obtained using methods from nonlinear system identification. In the context of this work we have developed a new algorithm for the identification of the *qualitative dynamics* of driven oscillatory systems. The method is advanced mathematically and sophisticated in its numerical implementation, so that a detailed description would by far exceed the scope of this paper. Thus, we will only describe the basic ideas here and refer to further publications with respect to the technical details.

The quantitative comparison of nonlinear models with experimental time series is complicated by a problem which is sometimes called the 'realization problem' (Sontag 1990). Many nonlinear model structures may be compatible with specific input/output time series. This makes reliable identification of the model impossible for a finite amount of data unless further restrictions are imposed on the fitted nonlinear model structure. We present a solution to this problem which is particularly tailored to answer the question whether the system dynamics contains essentially nonlinear contributions. The basic idea is to restrict the model ansatz to the normal form of the vector field of the relevant bifurcation, in our case the Hopf bifurcation (cf. Arrowsmith and Place 1990). This ansatz is optimally suited to finding the minimum number of essentially nonlinear terms that is necessary to capture the system behavior. In practice, the system is transformed into a new coordinate system that eliminates all nonlinear terms in the model which are not necessary for the qualitative dynamics.[5] Because the postural trajectories by themselves are very harmonic in shape, a linear transformation is assumed to be adequate.[6]. Introducing the new complex variable $z = \kappa(x + i\,(\tilde{\alpha}x/(2\omega_r) + \dot{x}/\omega_r)$, where $\omega_r = \sqrt{[\omega_0^2 - (\tilde{\alpha}/2)^2]}$ and $\kappa \in \mathbb{R}\backslash\{0\}$ is a scale factor, the transformed nonlinear dynamics can be written:

$$\dot{z} = -i\omega_r z + \sum_{k=1}^{K} c_k |z|^{2k} z + i\frac{\kappa}{\omega_r}\left[c_{\mathrm{env}}\omega_D \frac{D_r}{D_0}\cos(\omega_D t - \psi) + \sqrt{Q}\,\xi_t\right] \tag{7}$$

The linear part of this equation can easily be shown to correspond exactly to the linear model (3) considered earlier (cf. Hirsch and Smale 1974). By using methods similar to Schöner (1991) the effects of the nonlinear terms on the amplitude and phase dynamics can be analyzed. For instance, a nonlinear term of the form $i\,\mathrm{Im}\{c_1\}|z|^2 z$ effectively changes the eigenfrequency in (4) and (5) and leaves the stability properties and the relaxation time invariant.

5.1 Methods

The crucial technical problem is the dependence of the coordinate transformation on the fitted model parameters $\tilde{\alpha}$ and ω_0 themselves. The identification algorithm is based on a combination of a stepwise regression procedure (Kortmann 1988) and a nonlinear optimization procedure for the coordinate transformation between physical and the normal-form coordinates. The nonlinear optimization procedure minimizes an error functional that rewards good overall fit and good fit of the transient parts of the data and penalizes the introduction of nonlinear terms into the model. The real factor κ in the coordinate transformation is chosen to scale the stationary mean amplitude of the signal z in normal-form coordinates to 1. After the estimation of the linear model part, which was described in Sect. 4, the nonlinear terms are introduced step by step in increasing order of nonlinearity. In this way a model in normal form with a minimum order of the nonlinearity is estimated. A term was retained only if it contributed more than 5% to the remaining unexplained variance. The regression stopped when the model error first differed by less than 0.1% from the minimal error obtainable by introducing all nonlinear terms up to order 4 into the model or when the F values[7] of the fits of the real and the (more noisy) imaginary parts of $\dot{z}$ exceeded 1000 and 100, respectively. By identifying simulated data we verified that the procedure reliably detects nonlinear terms for oscillator structures with small and medium degrees of nonlinearity.

[5] The transformation leaves the qualitative dynamics of the system invariant, which means the original and the transformed system are topologically equivalent (see Arrowsmith and Place 1990, for further details).

[6] The general normal-form theorem (Arrowsmith and Place 1990) assumes a polynomial coordinate transformation. In our case this transformation would effectively change nonharmonic oscillatory solutions into harmonic ones. Nonharmonic solutions have never been observed experimentally.

[7] F was defined as the quotient of explained variance and error-variance.

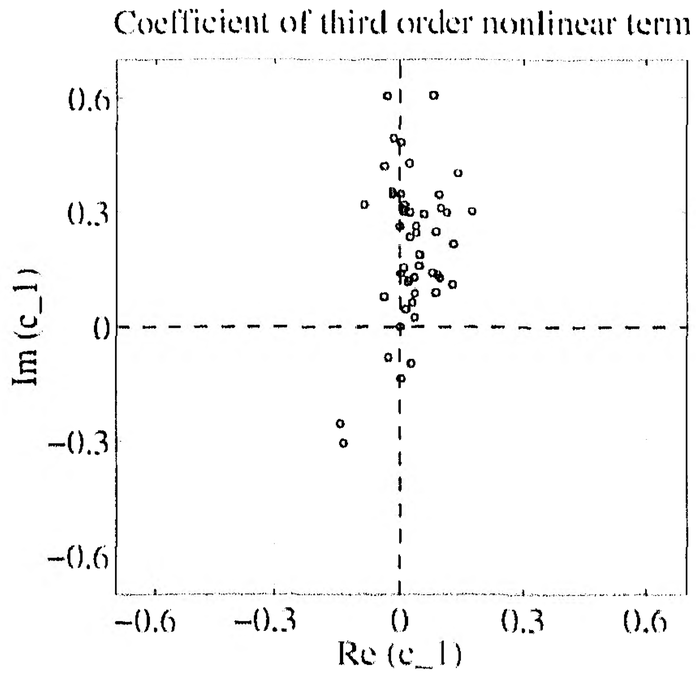

Fig. 10. Real (x-axis) and imaginary (y-axis) parts of the complex parameter c_1 of the nonlinear term $|z|^2 z$ as determined by fitting trajectories. The plot combines the values from all six subjects

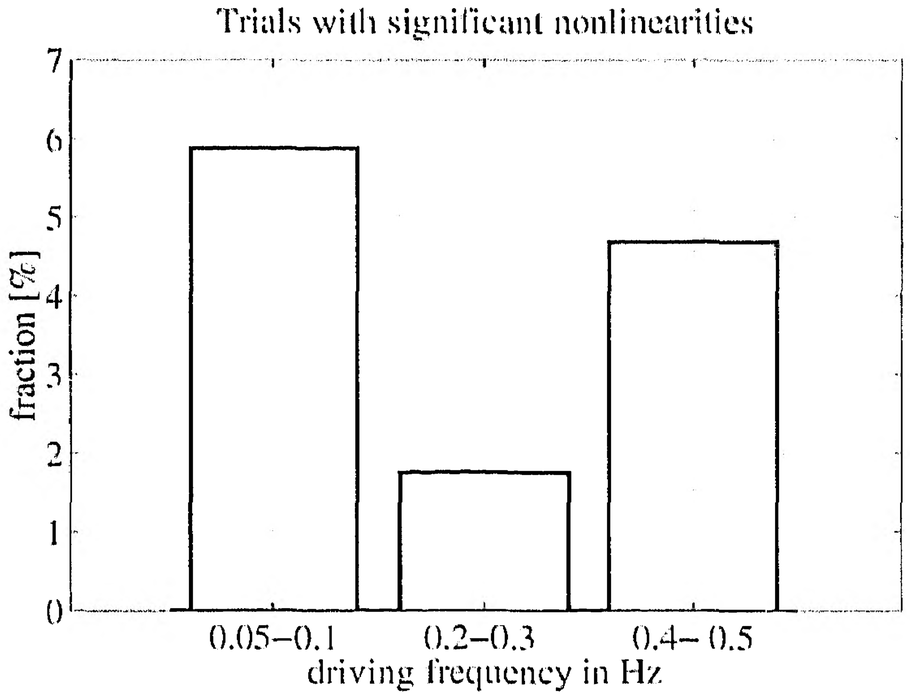

Fig. 11. Distribution of the significant nonlinear terms over different ranges of driving frequency. The figure shows the percentage of fitted trajectory segments with a significant nonlinearity of any order separately for the frequency conditions: 0.05 and 0.1 Hz, 0.2 and 0.3 Hz, 0.4 and 0.5 Hz. The plot combines the results for all six subjects

5.2 Results and discussion

Applied to the data, the variance of the *time series* explained by the fitted model ranged from 50% to 87%, and was typically 80%. We found that nonlinear contributions to the dynamics can be reliably detected with this procedure. Moreover, the distribution over trials and subjects is concentrated on the lowest-order terms: the third-order term $|z|^2 z$ was significant in 14% of the trials, while higher terms were almost never significant ($< 3\%$). The real and imaginary parts of this lowest-order nonlinearity are shown in Fig. 10. The plot shows the values for all subjects in the Gaussian complex plane. The nonlinear terms are concentrated on the imaginary axis around a value of $c_1 \approx 0.3\, i$. Figure 11 shows the distribution of significant nonlinear terms over different ranges of the driving frequency. The smallest fraction of significant nonlinearities (1.8% of the relevant data-segments) occurred in the middle frequency range (0.2 and 0.3 Hz). For low and high driving frequencies we found significantly more nonlinearities (5.9% and 4.7% of the data-segments; $\chi^2_2 > 13.6$).

A mathematical analysis and simulations show that the third-order nonlinearity contributes to the amplitude stabilization for low driving frequencies. For high driving frequencies the effect is contrary to what would be expected for a limit cycle with amplitude stabilization. In this regime the reduction of the damping coefficient seems to be the crucial factor for the stabilization of the amplitude. The nonlinearity has no influence on the stability of the system. The occurrence of nonlinear terms was significantly correlated with the presence of relative or no coordination in the relative phase analysis for one subject ($\phi = 0.4$, $\chi^2_1 > 10$). Given the relatively rare occurrence of nonlinear terms and their reducing effect on amplitude for high stimulus frequencies our analysis shows no indications for a nonlinear limit-cycle dynamics as a crucial mechanism for the stabilization of the response amplitude. We conclude that a description as an adaptive linear system is more adequate than a description as an essentially nonlinear system.

6 General discussion

By comparing dynamical models with the postural sway trajectories induced by a rhythmically moving visual environment we found: (1) The amount of sway matched approximately the amount of visual motion at all frequencies. Note that this amount varied with frequency because we had adjusted the amplitude of visual motion to keep peak visual velocities constant. (2) Constant-parameter linear dynamical models fail to account for the data. In particular, these models are unable to accommodate the weak resonance effect observed at the levels of both phase and gain. (3) When the parameters of the linear dynamical model are allowed to depend on the frequency of visual motion, the data set can be consistently described. From this analysis the following account emerges: (a) The postural system adapts its proper frequency to closely match the visual frequency. In this way, the range of frequencies over which postural sway can remain coherent with the visual signal is greatly extended (cf. Dijkstra et al. 1994b). (b) The postural system actively destabilizes the postural state in the inertial frame by generating a negative damping. The contribution of vision is then sufficient to warrant overall stability. This reduction of the nonvisual contribution to postural stability enables the system to achieve sway amplitudes that continue to match visual motion amplitudes even beyond the boundaries of the normal dynamic range of postural sway. In a way, the system makes itself more susceptible to visual input by destabilizing its intrinsic postural state in the inertial frame. (4) Although the system has identifiable nonlinearities, these do not contribute to the qualitative dynamics of sway.

The first effect is consistent with similar observations reported in Dijkstra et al. (1994a), where amplitude of sway matched amplitude of the visual motion over a range of distances to the visual scene. Similarly, Talbott (1980) reported for dogs that their sway amplitude remains close to the amplitude of mechanical oscillations of the support platform over a comparable frequency range. These results are in contrast with reports by Lestienne et al. (1977) and van Asten et al. (1988a), who found a strong decrease of gain with frequency. This contrast is also evident with respect to the effect (2): while Lestienne et al. and van Asten et al. found the change from phase advance to phase delay with increas-

ing frequency which is characteristic for constant-parameter driven systems, we, like Talbott and Brookhart (1980), found constant parameter linear models to be inadequate, because the characteristic resonance structure was too weakly developed in the data.

One difference between the two sets of experiments is the scale of visual motion. We used small amplitudes that generate retinal slip not far removed from that occurring for normal postural movements in a resting visual world. (Fig. 2 shows that the active compensatory postural movements greatly reduce the expansion rates.) Similarly, Talbott (1980) applied mechanical perturbations within a range that can be compensated for by the animals. By contrast, van Asten et al. (1988a) used large amplitudes of visual motion (±30 cm and ±120 cm). In van Asten et al. (1988b) the visual motion was generated by rotating a scene periodically at ±17 deg while the achieved postural rotation at the ankle joint is of the order of ±2 to 3 deg. Lestienne et al. (1977) used either constant visual velocity or oscillation between rather strong values. The spatial significance of such large-scale visual motion is not entirely clear, but an object would have to move substantially to generate this type of velocity pattern on the retina. A possible explanation for the difference between the two sets of experiments is thus that in our experiment and Talbott's, visual motion specified a successful postural behavior strategy in the visual world, contrary to the experiments by Lestienne and van Asten. More concretely, in the first set of experiments it was possible for subjects to generate a sway that would lead to approximately zero visual motion. By contrast, for the large amounts of spatial movement underlying visual stimulation in the other experiments the visuomotor system does not provide a successful behavioral compensation strategy. This might be due to physical limitations of the motor system, or to the rare occurrence of situations where large-amplitude visual movements require postural readjustments. Under those circumstances, the system may remain unaffected in its internal structure by the specific external visual stimulation. The visual stimulus then may act essentially as a driving force for the system which has stimulus-independent internal parameters.

Our third observation can best be interpreted as evidence for adaptation. Because in the analyzed data segments no evidence was found for ongoing adaptation, this process must have taken place within the first 20 s of each trial, which have not been included in the analysis (exactly to warrant stationarity: see Dijkstra et al. 1994b). This is consistent with the time scale of adaptation reported in other studies (Schuster and Talbott 1980, Clement et al. 1985). Adaptation could underlie the generation of an internal representation or model of the external periodic motion as hypothesized, for instance, by Maioli and Poppele (1991). An interesting topic for further research would be the direct investigation of the adaptation process. A possible experimental strategy would be to record the changes in the dynamics immediately after a change of stimulus frequency or amplitude.

The presence of nonlinear contributions has been repeatedly proposed (for discussion see van Asten et al. 1988b), but has not been viewed as leading to qualitative change of the postural dynamics, consistent with our findings. However, we should point out that we investigated nonlinear contributions to the dynamics of the postural system coupled to a time-variant visual environment. By contrast, more substantial nonlinear contributions might be observable within a single integrated postural control system in a temporally invariant environment. For instance, Collins and De Luca (1993, 1994) found two different dynamic regimes during quiet standing, which might well be related to a dynamic instability in which the linear contribution vanishes and the nonlinear contribution dominates.

The most concise summary of our results is that the generation of postural sway in a moving visual environment is an active process rather than a passive response to the input. In Sect. 1 we raised the general question of how an analysis of the postural system can proceed in the face of experimental evidence for adaptive change and active generation of sway. From our work we would draw three conclusions relative to this question: (i) A detailed quantitative assessment of the postural system is necessary to uncover its actual structure. For instance, in our work the results of the frequency manipulation are superficially consistent with linear constant-parameter models. Only quantitative work detected the discrepancy and can help to identify the active mechanism of adaptation. (ii) Such quantitative work is strong and leads to interpretable results if the choice of variables is guided by the behaviors that emerge in the system, rather than by putative sensor or effector variables. Analysis of a given behavior then means to identify an dynamical system at the level of such variables, that accounts for observed behaviors as dynamically stable solutions (Schöner and Kelso 1988). For instance, in our work the functional significance of the adaptive changes was interpretable because it was directly analyzed in terms of the stability of the postural state in the inertial frame (parameter α) or in the visual world (parameter $\tilde{\alpha}$). (iii) For the analysis of a postural system, the conditions to which the system is exposed in an experiment must be chosen and controlled with respect to a specified behavior. A continuous change in stimulus conditions can lead to a categorical change with respect to what is specified. For instance, increasing the amplitude of visual motion may lead a system from a regime in which successful postural stabilization in the visual world is possible, to a regime in which such visual motion acts merely as a perturbation of an otherwise passive system.

Taken together, these hypotheses would suggest looking for an entirely different strategy of analysis of the postural system. Rather than analysing the postural response as function of parameters of the peripheral sensory information, one would aim to discover different elementary behaviors which can be induced by providing the adequate sensory and task environment. These behaviors may occur in discrete regimes of the specifying parameters. For instance, stabilization of posture in the visual world and stabilization of posture in the inertial world could be two such elementary behaviors. We found that posture stabilization in the visual world dominates when weak visual motion is applied. It is conceivable that a much richer set of behaviors can be observed at the level of posture, however. For instance, posture may relate to other movement tasks by stabilization against the mechanical perturbations induced by such movements or by actively taking part in such movements by providing momentum. Onset of locomotion, preparation to jump, etc., might require differ-

ent patterns of control. Analysis would then mean identifying such behaviors, to determine the corresponding control dynamics of the postural system, and to understand how the behaviors interact (e.g., compete or cooperate).

Acknowledgements. This work was supported by the Studienstiftung des deutschen Volkes, the Foundation for Biophysics, MUCOM (ESPRIT BRA 3149 and 6615) and by MWF, Düsseldorf. The valuable comments of K. Kopecz and J. Jeka are gratefully acknowledged. We especially thank C. Schmid for several interesting discussions. We would like to thank A. Steinhage and T. Lau for their assistance.

References

Arrowsmith DK, Place CM (1990) An introduction to dynamical systems. Cambridge University Press, Cambridge

Asten WNJC van, Gielen CCAM, Denier van der Gon JJ (1988a) Postural adjustments induced by simulated motion of differently structured environments. Exp Brain Res 73:371–383

Asten WNJC van, Gielen CCAM, Denier van der Gon JJ (1988b) Postural movements induced by rotations of visual scenes. J Opt Soc Am A 5:1781–1789

Bohr T, Bak P, Jensen MH (1984) Transition to chaos by interaction of resonances in dissipative systems. II. Josephson junctions, charge-density waves, and standard maps. Phys Rev A 30:1970–1981

Clement G, Jacquin T, Berthoz A (1985) Habituation of postural readjustments induced by motion of visual scenes. In: Igarashi M (ed) Vestibular and visual control on posture and locomotor equilibrium. Karger, Basel, pp 99–104

Collins JJ, De Luca CJ (1993) Open-loop and closed-loop control of posture: a random-walk analysis of center-of-pressure trajectories. Exp Brain Res 95:308–318

Collins JJ, De Luca CJ (1994) Random walking during quiet standing. Phys Rev Lett 73:764–767

Dichgans, J, Brandt T (1978) Visual-vestibular interaction: effects on self-motion perception and postural control. In: Held R, Leibowitz HW, Teuber HL (eds) Perception. Springer, Berlin Heidelberg New York, pp 755–804

Dijkstra TMH, Schöner G, Gielen CCAM (1994a) Temporal stability of the action-perception cycle for postural control in a moving visual environment. Exp Brain Res 97:477–486

Dijkstra TMH, Schöner G, Giese MA, Gielen CCAM (1994b) Frequency dependency of the action-perception cycle for postural control in a moving visual environment: relative phase dynamics. Biol Cybern 71:489–501

Halfon E, Unbehauen H, Schmid C (1979) Model order estimation and system identification: theory and application to the modelling of ^{32}P kinetics within the tropogenetic zone of a small lake. Ecol Modelling 6:1–22

Hirsch MW, Smale S (1974) Differential equations, dynamical systems, and linear algebra. Academic Press, New York

Holst E von (1937/1973) On the nature of order in the nervous system. In: Martin R (transl.) The behavioural physiology of animals and man, vol 1. Methuen, London

Horak FB, Diener HC, Nashner LM (1989) Influence of central set on human postural responses. J Neurophys 62:841–853

Ishida A, Miyazaki S (1987) Maximum likelihood identification of a posture control system. IEEE Trans Biomed Eng 34:1–5

Kortmann M (1988) Die Identifikation nichtlinearer Ein- und Mehrgrössensysteme auf der Basis nichtlinearer Modellansätze. VDI Verlag, Düsseldorf

Lestienne F, Soechting J, Berthoz A (1977) Postural readjustments induced by linear motion of visual scenes. Exp Brain Res 28:363–384

Maioli C, Poppele RE (1991) Parallel processing of multisensory information concerning self- motion. Exp Brain Res 87:119–125

Maki BE, Holliday PJ, Fernie GR (1987) A posture control model and balance test for the prediction of relative postural stability. IEEE Trans Biomed Eng 34:797–810

Marple SL (1987) Digital spectral analysis with applications. Prentice-Hall, Englewood Cliffs, NJ

Massion J (1992) Movement, posture, and equilibrium: interaction and coordination. Prog Neurobiol 38:35–56

Nashner LM, McCollum G (1985) The organisation of human postural movements: a formal basis and experimental synthesis. Behav Brain Sci 8:135-172

Paulus W, Straube A, Krafczik S, Brandt T (1989) Differential effects of retinal target displacement, changing size and changing disparity in the control of anterior/posterior and lateral body sway. Exp Brain Res 78:243–252

Press WH, Flannery BP, Teukolsky SA, Vetterling WT (1988) Numerical recipes in C. Cambridge University Press, Cambridge

Riccio GE, Stoffregen TA (1991) An ecological theory of motion sickness and postural instability. Ecol Psychol 3:195–240

Schöner G (1991) Dynamic theory of action-perception patterns: the 'moving room' paradigm. Biol Cybern 64:455–462

Schöner G, Kelso JAS (1988) Dynamic pattern generation in behavioral and neural systems. Science 239:1513–1520

Schuster D, Talbott RE (1980) Optimal and adaptive control in canine postural regulation. Am J Physiol 239:R93–R114

Sontag ED (1990) Mathematical control theory. Springer, Berlin Heidelberg New York

Talbott RE (1980) Postural reactions of dogs to sinusoidal motion in the peripheral visual field. Am J Physiol 239:R71–R79

Talbott RE, Brookhart RE (1980) A predictive model study of the visual contribution to canine postural control. Am J Physiol 239:R80–R92